P1.11 NUMERICAL INVESTIGATION OF INTERNAL WAVE-VORTEX INTERACTIONS

Tyler D. Blackhurst and J. C. Vanderhoff *
Brigham Young University, Provo, Utah

1. INTRODUCTION

A stably-stratified fluid is one in which the density increases continuously with depth, such as the ocean or the atmosphere. Perturbations of a stably-stratified fluid, such as winds over topography, move fluid particles of one height and neutrally-buoyant state to a height in which they are surrounded by fluid particles of a different density. Oscillations less than the natural frequency create internal waves which play an integral role in oceanic and atmospheric dynamics.

Numerical methods are common for simulating internal wave propagation and wave interactions with other fluid phenomena, studying them from every point in space and time, and comparing the results with what is known from observation and experimentation. However, reconciling theoretical predictions with experimental data is sometimes problematic since, during wave propagation and interactions, the transport of energy may be at such small scales that observations lack sufficient resolution and the onset of turbulence invalidates two-dimensional linear theories. With three-dimensional-simulation capabilities, we can more completely study scenarios involving internal waves in the ocean and atmosphere and apply more accurate theories and approximations.

Internal waves interact with a myriad of flow phenomena, including other internal waves of similar and different scales. Javam, Imberger, and Armfield (2000) numerically researched interactions of internal waves of similar scales and found these interactions were nonlinear and involved wave breaking. Broutman and Young (1986) used ray theory (to be described later) to numerically track the changes of small-scale internal waves (on the order of tens of meters) interacting with a large-scale internal wave background (on the order of kilometers and greater). They confirmed theoretical predictions for conditions of internal waves prior to and following the interactions. Winters and D'Asaro (1989) used a two-dimensional model to numerically simulate the propagation of internal waves into a slowly-varying mean shear background. Nonlinearity and three-dimensionality overcome the simulated waves when the internal waves become unstable and turbulence begins, breaking down the internal waves. Later, three-dimensional considerations were discussed in Winter and D'Asaro (1994). Convective instabilities yielded counter-rotating vortices, the effects of which were magnified by wave shear. The combination of convection and shear in these interactions obligate three-dimensional analysis. This obligation is a representative result of all the studies cited thus far and is essential to the continuing discussion.

Vortices are a common occurrence in large, geophysical flows as a result of shear and turbulence in a rotating fluid. Moulin and Flór (2006) numerically demonstrated a three-dimensional interaction between a large-scale internal wave and a Rankine-type vortex. By varying the initial locations of the internal waves, the authors demonstrated that each wave-vortex interaction resulted in a different scenario with different effects on the internal waves. In some cases, the waves reflected; in others, they were absorbed into the rotating flow; still other combinations produced breaking waves. Despite the wealth of information gained from these simulations, questions remain about what happens to the energy of internal waves during the onset of turbulence and other three-dimensional characteristics during wave-vortex interactions. While we know the waves may break, it is unclear what mechanisms are responsible for their evolution to breaking and how and why turbulence begins.

Godoy-Diana, Chomaz and Donnadieu (2006) discussed the experimental interaction of internal waves with a Lamb-Chaplygin pancake vortex dipole, an exact solution of the Euler equations (Billant, Brancher, and Chomaz (1999)). A vortex dipole involves two side-by-side, counter-rotating vortices. Two scenarios of wave-vortex interactions were conducted: one in which the internal wave's horizontal group speed propagated with the flow and one in which it propagated against the flow. The former scenario showed the wave beam bending to the horizontal and being

* *Corresponding author address:* Tyler D. Blackhurst, Brigham Young University, Dept. of Mechanical Engineering, Provo, UT, 84602; email: tyblackhurst@byu.edu.
J. C. Vanderhoff, Brigham Young University, Dept. of Mechanical Engineering, Provo, UT, 84602; email: jvanderhoff@byu.edu.

absorbed by the vortex, yielding its energy to the dipole. The latter scenario resulted in the beam of internal waves steepening to the vertical and possibly reflecting. The results of this experiment suggest three-dimensional effects are essential in understanding this type of interaction. A numerical analysis of this experiment illuminates the three-dimensional mechanisms of these effects, showing what happens to the internal wave properties and energy. It gives insight into possible interactions that may lead to wave breaking and turbulence.

This paper details the work that has been done and discusses work to still be done to numerically model a set of small-scale internal waves interacting in three dimensions with a vortex dipole of constant translational speed. Section 2 relates the experimental setup of Godoy-Diana *et al.* (2006) and the corresponding numerical setup for the current study, including the mathematical theory involved. Section 3 presents and discusses the results of the interaction simulations, including comparisons to the experiment of Godoy-Diana *et al.* (2006). Section 4 considers the practical impact of this numerical study, summarizing its results and expected further research.

2. METHODS

The experimental internal wave-vortex interaction of Godoy-Diana, *et al.* (2006) was completed in a salt-stratified water tank, the setup of which is sketched in Figure 1. The dipole was created by closing two flaps at one end of the tank. The dipole approached a screen which allowed only a thin slice of the dipole to pass into the test section of the tank. The internal-wave beams were generated by oscillating a cylinder at a frequency less than the natural buoyancy frequency of the fluid. Figure 2 shows a close-up view of the two experimental interactions of Godoy-Diana, *et al*. (2006): co-propagating, for which the waves propagated in the same direction as the translating vortex dipole; and counter-propagating, for which the waves propagated in a direction opposite to the translating vortex dipole. In both cases, the wave beams are generated along the axis of the dipole. The expected outcome of the experiment can be seen as the co-propagating wave beam is absorbed into the flow of the dipole at a critical level (defined as the depth where the relative frequency of the internal waves equals the natural buoyancy frequency of the fluid), and the counter-propagating representation of the wave beam is reflected away from the dipole at a turning point (defined as the depth where the relative frequency of the internal waves approaches zero).

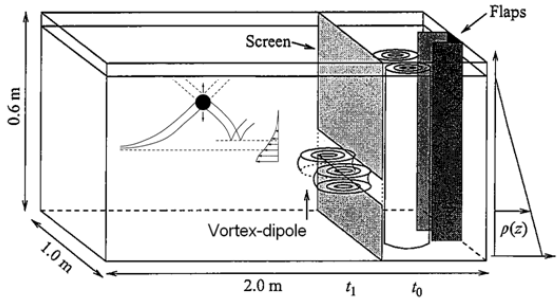

Figure 1: Saltwater-stratified experimental tank (Godoy-Diana et al. (2006)). The dipole was created by flaps at one end of the tank and approached a screen which allowed a slice of the dipole to pass into the test section of the tank where a horizontal cylinder generated internal waves.

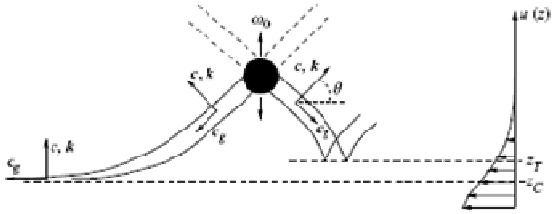

Figure 2: Close-up view of oscillating cylinder generating internal waves relative to the dipole's vertical velocity profile (Godoy-Diana, et al. (2006)). The internal waves were generated along the axis of the dipole. The co-propagating case shows the internal waves being absorbed by the dipole at a critical level (z_C). The counter-propagating case shows the internal waves reflecting off the dipole at a turning point (z_T).

The numerical code for the current study was written in Matlab. It has been modified from a two-dimensional code and developed for three-dimensional simulations. At the code's core, ray theory governs the numerical simulation. Ray theory, often called ray tracing, traces the directions of internal-wave energy propagation before, during, and after the wave-vortex interaction. Ray theory is linear, so the basic propagation of the waves can be simply modeled. In addition, calculations can be made to analyze wave amplitudes which may result in wave breaking and possibly lead to turbulence. Ray theory is quick in its application, providing a method of research much faster and less expensive than experimentation, observation, and fully nonlinear numerical simulations.

Ray theory is a method of solving the Navier-Stokes equations, the governing equations of fluid flow. To simplify the Navier-Stokes equations for this case, the translation of the vortex is assumed slowly varying while the only side-effects of the

interaction are changes to the characteristics of the small-scale internal waves. This is the linear, inviscid Wentzel-Kramer-Brillouin (WKB) approximation. It is the foundation of ray theory, allowing the dispersion relation (see Equation (2) below) to be locally valid. While it is not representative of all wave-vortex interactions, this assumption is realistic when waves are interacting with large-scale geophysical flows. Another simplification is the Boussinesq approximation, which states that changes in density are negligible except in terms where the acceleration due to gravity is a multiplier. The solution to the Navier-Stokes equations is then in a form of the wave equation.

The complete ray theory equations for a mean velocity field $\boldsymbol{V}= (v_1,v_2,v_3)$ through which the internal waves propagate with frequency relative to the background are now presented.

The Doppler relation defines the relation between the frequencies of the background Ω and the intrinsic frequency of the internal wave ω_r,

$$\omega_r = \Omega - v_j k_j \tag{1}$$

where v_j is the component of the background velocity and k_j is the component of the small-scale wavenumber vector $\boldsymbol{k}= (k_1,k_2,k_3)$ in the same direction. The dispersion relation defines ω_r as a function of wavenumber, the buoyancy frequency N, and the Coriolis force (which is insignificant for the simulations at hand),

$$\omega_r^2 = \frac{N^2(k_1^2+k_2^2)+f^2m^2}{k_1^2+k_2^2+k_3^2} \tag{2}$$

The velocities of the internal waves are defined by the sum of the background velocity and the group velocity of the internal waves,

$$\frac{dx_i}{dt} = v_i + \frac{\partial\omega}{\partial k_i} \tag{3}$$

for which $\boldsymbol{x}=(x_1,x_2,x_3)$ defines the space of the domain and where the group velocity is given by

$$\frac{\partial\omega_r}{\partial k_i} = (N^2-1)k_i \frac{\left[N^2(k_1^2+k_2^2)+f^2k_3^2\right]^{1/2}}{(k_1^2+k_2^2+k_3^2)^{3/2}} \tag{4}$$

The law governing refraction is given by

$$\frac{dk_i}{dt} = -k_j \frac{\partial v_j}{\partial x_i} - \frac{\partial\omega_r}{\partial x_i} \tag{5}$$

To define the change of the relative frequency with respect to time,

$$\frac{d\omega_r}{dt} = \frac{\partial\omega_r}{\partial k_i}\frac{dk_i}{dt} + \frac{\partial\omega_r}{\partial x_i}\frac{dx_i}{dt} \tag{6}$$

For this simulation, the partial derivative of ω_r with respect to space is zero because $\boldsymbol{k}$, N, nor f in the dispersion relation is a function of space. Thus the right hand sides of the last two equations reduce to only their first terms.

In order for ray theory to trace the interactions, the numerical vortex dipole was created following the equations for a Lamb-Chaplygin vortex dipole set forth by Billant, *et al*. (1999). Inside the dipole, the stream function and axial vorticity are defined respectively as

$$\psi_0(r,\theta) = -\frac{2UR}{\mu_1 J_0(\mu_1)} J_1(\mu_1 \frac{r}{R})\sin\theta \tag{7}$$

$$\omega_{z0} = -\frac{\mu_1^2}{R^2}\psi_0 \tag{8}$$

Outside the dipole they are

$$\psi_0(r,\theta) = -Ur\left(1-\frac{R^2}{r^2}\right)\sin\theta \tag{9}$$

$$\omega_{z0} = 0 \tag{10}$$

In Equations (7) through (10), U is the translating velocity of the dipole, R is the dipole radius, J_0 and J_1 are the zero- and first-order Bessel functions, and μ_1 = 3.8317 is the first zero of J_1. The numerically-generated vortex dipole is shown in Figure 3 as if one were looking from above into the tank with the dipole translating right to left. The vectors represent qualitatively the magnitude and direction of the velocity at that point in space. The velocity profile along the depth of the vortex dipole is a normal Gaussian curve and is given in Figure 4.

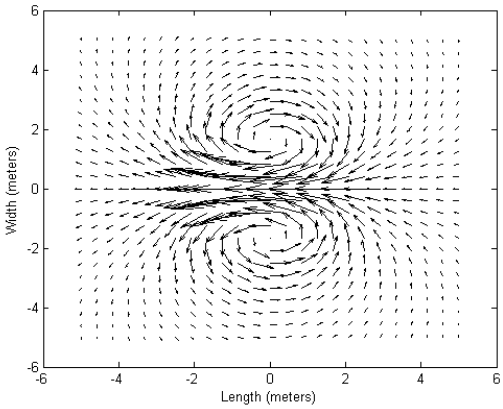

Figure 3: Lamb-Chaplygin vortex dipole. The vectors represent qualitatively the magnitude and direction of the velocity at that point in space.

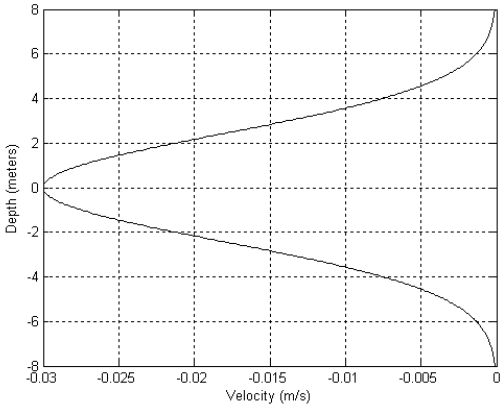

Figure 4: Velocity profile along the depth of the vortex dipole.

3. RESULTS AND DISCUSSION OF RESULTS

To validate the results of the numerical simulations, they are compared to the experimental results of Godoy-Diana, *et al.* (2006). Figure 5 shows four images taken during the experiment, demonstrating the evolution of the co-propagating scenario. Figure 5a shows the beams of internal waves before interaction with the dipole. Figure 5b shows one of the beams bending to the velocity profile of the dipole. Figures 5c and 5d show the beams being absorbed by the vortex.

Figure 6 shows a possible wave-vortex interaction done numerically in a three-dimensional domain. The lines are rays traced for various internal waves. The waves begin at the same position along the length and along the depth of the domain, but at different positions along the width. They also begin with the same wave numbers. The center ray may be directly compared to Godoy-Diana, *et al*. (2006).

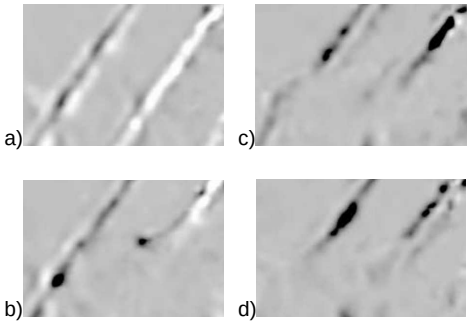

Figure 5: View of co-propagating experimental results from Godoy-Diana, *et al.* (2006) showing the wave beams changing along the depth with respect to the length of the tank. a) shows the internal wave beams prior to the interaction; b) shows one wave beam being absorbed; c) and d) show the evolution of the interaction as the dipole absorbs the wave beams.

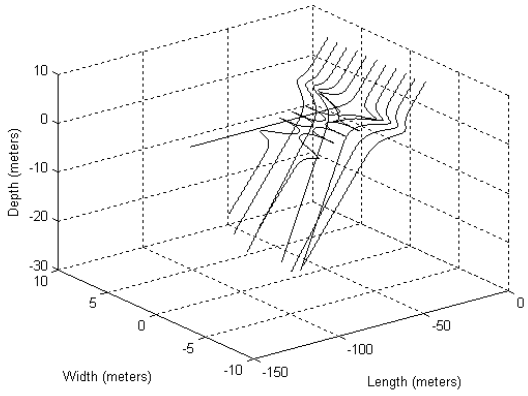

Figure 6: Three-dimensional view of the numerical co-propagating simulation. The lines are the rays traced by ray theory and represent internal waves over time. They begin at the same position along the length and the depth in the domain, but at different positions along the width. The center ray is seen absorbed by the dipole at a critical level.

The rays follow the patterns expected in an interaction with a vortex dipole over time. Most of the off-center rays interacted briefly before escaping the dipole, while two in particular were caught for a time in the circulation of the vortices before escaping. The center ray was absorbed by the vortex dipole as it reached a critical level, as in Godoy-Diana *et al*. (2006) (see Figure 5). This can be more clearly seen in Figure 7, plotting the rays with respect to depth and a nondimensional time t / T_N, where T_N is the natural buoyancy period of the fluid. In this figure, the center ray (top) is shown first interacting with the dipole near 3 meters in depth. Its slope flattens to zero once the critical level is reached at approximately 2.5 meters. There the internal waves yield their energy to the dipole.

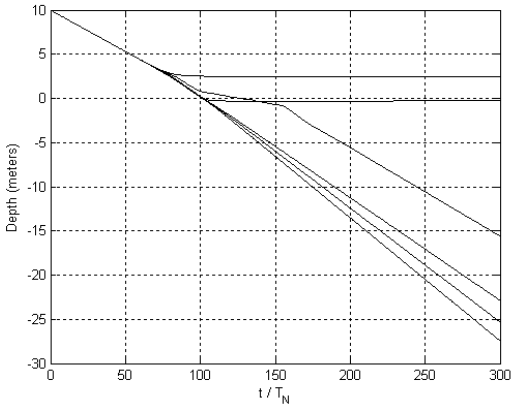

Figure 7: View of numerical solution showing how rays change along the depth with respect to a nondimensional time t/T_N, where T_N is the natural buoyancy period of the fluid. The top ray is the center ray of Figure 6, and is entirely absorbed by the dipole at a critical level. Off-center rays escape the dipole at angles different than before the interaction, some nearing a slope of zero but not quite reaching a critical level.

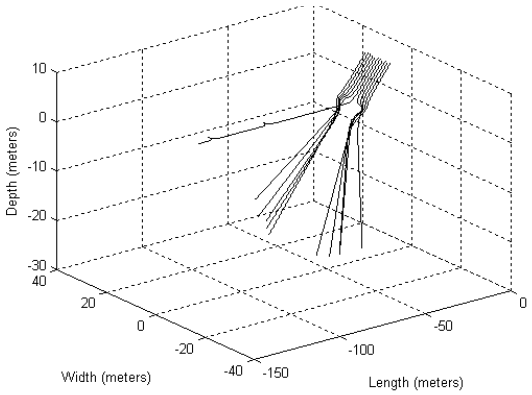

Figure 8: Results of numerical simulation accounting for time changes of all wavenumber vector components. The off-center rays spread more than previously. The center ray again reaches a critical level, but now has small, periodic perturbations in the horizontal.

The numerical simulation above does not account for all three components of the wavenumber vector. The time dependence of k_2 according to Equation (5) was neglected, holding k_2 constant throughout the simulation. The following numerical simulations demonstrate three-dimensional effects of wave-vortex interactions and, when compared to the previous simulation, show the import of fully three-dimensional numerical simulations.

The first results of a simulation incorporating the time-change of k_2 is shown in Figures 8 and 9. The initial positions of the rays remained the same as the previous simulation, as did the initial value of the wavenumber vector. Figure 8 is a three-dimensional view showing greater refraction of the off-center rays as they exit the interaction than when the third dimension is neglected. Their spreading is more significant, acknowledging a transfer of energy among wavelengths.

The center ray is again absorbed by the dipole, as can be confirmed in Figure 9, plotting a nondimensional time against the depth. However, in the horizontal, the center ray has periodic perturbations. As a check, the first simulation was rerun to allow the rays more time to propagate. It was found that the center ray was also perturbed in this earlier example. As will be shown in the next example, this seems to be an effect of the relative positioning in the length of the rays to the dipole.

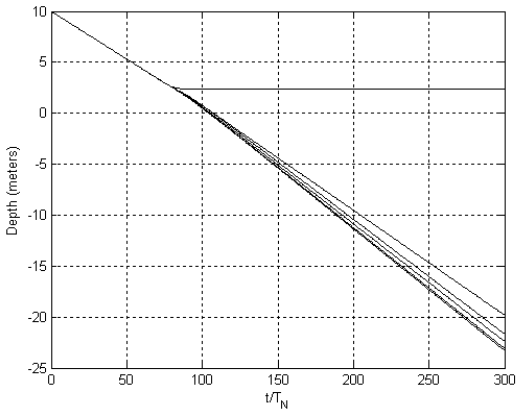

Figure 9: Ray propagation along the depth plotted in a nondimensional time. This simulation incorporated time changes of the wavenumber vector in all three dimensions. The center ray of the interaction is seen reaching the critical level, as before, near 2.5 meters.

The initial positions of the rays in the next simulation are different than the previous two only along the length of the domain, beginning nearer to zero by more than 10 meters. The initial wavenumber vector remained unchanged. The change in initial position affected the position of earliest interaction between the waves and dipole. In this case, the waves interacted with the dipole farther back along the length of the domain.

Significant spreading still occurred among the off-center rays, as can be seen in Figure 10. However, the center ray, which has been bolded for convenience, was not absorbed by the dipole. This is confirmed by plotting the depth of the rays against a nondimensional time in Figure 11. The center ray is the higher ray on the plot. Its slope flattens, but only slightly. As it never reaches a

critical level, it does not lose its energy to the dipole.

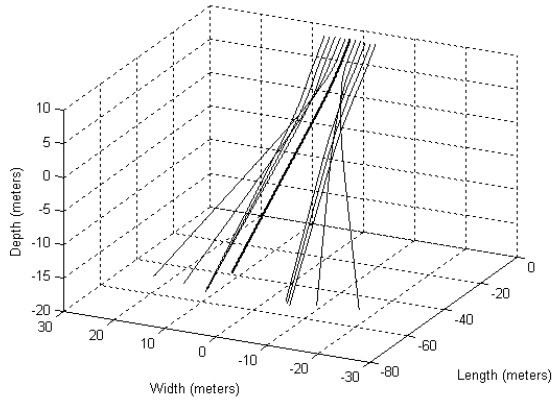

Figure 10: The rays are more than 10 meters nearer to zero in the length than the previous simulations. The off-center rays briefly interacted and spread as before. The center ray, in bold, was not absorbed by the dipole.

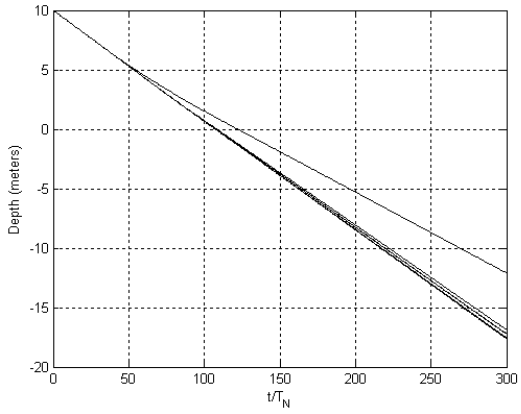

Figure 11: The depth of rays plotted against a nondimensional time. With the initial position of the rays along the length of the domain farther back relative to the dipole than before, the center ray did not reach a critical level.

Though the center ray did not reach a critical level in this scenario, neither did it have any perturbations in the horizontal. Figure 12 shows a view of the domain from one end of the tank where the dipole is translating out of the page. It can be clearly seen that the center ray never verged from the dipole axis. This appears to indicate that the perturbations seen in the previous simulations are results of the initial positioning of the rays.

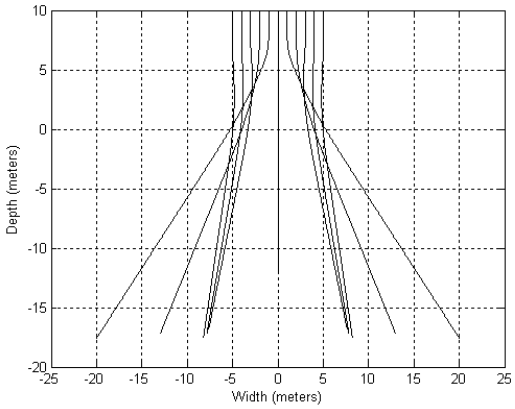

Figure 12: View of wave-vortex interaction from end of tank, with the vortex dipole translating out of the page. With the initial positions of the rays beginning nearer to zero in the length, the interaction began farther back on the dipole. The center ray was never perturbed.

4. CONCLUSION

Several points of interest have arisen from this study. First, the impact of utilizing all three dimensions of the wavenumber vector is shown in a comparison of the first numerical simulation with the second. The difference is seen qualitatively in comparing the spreading of the off-center rays; they spread more significantly when all three components of the wavenumber vector are affected in time due to the interaction. This confirms thoughts shared by Godoy-Diana, *et al*. (2006) regarding the importance of three dimensions in wave-vortex interactions.

Second, with the fully three-dimensional simulations, it is interesting to note the relative spreading of the rays depending on their initial locations. The third simulation initialized the rays approximately 10 meters nearer to zero in the length than the second simulation. As a result, the wave-vortex interaction occurred farther back relative to the dipole. The spreading of this simulation was less than that of the second, in which the rays interacted with the dipole nearer to its center. The greater spreading is a sign of greater energy transfer among the wavelengths. This may be significant when considering relative wave amplitudes in regards to breaking and turbulence and the prediction of their times and locations of occurrence.

Finally, the initial location of the ray in line with the dipole axis also seems to affect the solution of that ray's interaction with the dipole. The third simulation showed the center ray moving directly along the plane of the dipole axis. Though not absorbed, it didn't vary in the horizontal. In the

second simulation (also mentioned with the first), the center ray had unexpected perturbations in the horizontal even though it was fully absorbed by the dipole at the critical level. Other possible explanations for this include potential breaking, in which case analyses involving the wave energy and amplitude would imply such. Also, it may be a numerical bug making zero a very small but nonzero value. Currently, work is being done to determine the true reason.

Further work includes modifying the current code to simulate the counter-propagating wave-vortex interaction. With both experiments of Godoy-Diana, *et al*. (2006) numerically set, work will begin to evaluate wave energies and amplitudes and to modify initial conditions with the ray properties, not just locations. This will lead to conditions that result in wave breaking. Also, work will be done to parameterize the code so that numerical simulation may be done on large scales.

5. REFERENCES

Billant, P., Brancher, P., & Chomaz, J., 1999: Three-dimensional stability of a vortex pair. *Phys. Fluids*, 11, 2069-2077.

Broutman, D. & Young, W.R., 1986: On the interaction of small-scale oceanic internal waves with near-inertial waves. *J. Fluid Mech.*, 166, 341-358.

Godoy-Diana, R., Chomaz, J., & Donnadieu, C., 2006: Internal gravity waves in a dipolar wind: A wave-vortex interaction experiment in a stratified fluid. *J. Fluid Mech.*, 548, 281-308.

Javam, A., Imberger, J., & Armfield, S.W., 2000: Numerical study of internal wave-wave interactions in a stratified fluid. *J. Fluid Mech.*, 415, 65-87.

Moulin, F.Y. & Flór, J.-B., 2006: Vortex-wave interaction in a rotating stratified fluid: WKB simulations. *J. Fluid Mech.*, 563, 199-222.

Winters, Kraig B. & D'Asaro, Eric A., 1989: Two-Dimensional Instability of Finite Amplitude Internal Gravity Wave Packets Near a Critical Level. *J. Geophys. Res.*, 94, 12,709-12,719.

Winters, Kraig B. & D'Asaro, Eric A., 1994: Three-dimensional wave instability near a critical level. *J. Fluid Mech.*, 272, 255-284.